Mechanism and optimization of metal deposition onto vertically aligned single walled carbon nanotube arrays

Hai M. Duong, Kei Ishikawa, Jun Okawa, Kazuaki Ogura, Erik Einarsson, Junichiro Shiomi,

*Shigeo Maruyama**

Department of Mechanical Engineering, The University of Tokyo

7-3-1 Hongo, Bunkyo-ku, Tokyo 113-8656, Japan

*Author email: maruyama@photon.t.u-tokyo.ac.jp ; TEL/FAX: +81-3-5841-6421 / +81-3-5800-6985

ABSTRACT Arrays of vertically aligned single-walled carbon nanotubes (VASWNTs) were coated with thin films of Ti, Pd, Au, and Al by evaporative deposition. Scanning electron microcopy (SEM) showed the Ti and Pd coatings were continuous or quasi-continuous, while Au and Al agglomerated into discrete deposits on SWNT bundles. The mechanism of metal film formation on VASWNT arrays was studied by observing the film at various stages of the depositing process. Uniformity of the deposition was found to be strongly dependent on the metal species and the deposition conditions, such as substrate temperature, deposition rate, and deposition thickness. The optimization of the deposition conditions was demonstrated for Pd. The results suggest that the deposition efficiency for smooth coating layer is determined by the balance of two processes with significantly different speed; the coating along an SWNT-bundle and coating of an inter-bundle, which depend on the metal type and the deposition conditions. These findings may be useful regarding both fundamental and practical aspects of VASWNT applications in thermal and electronic devices.

Keywords: Single-walled carbon nanotube, Carbon nanotube film, Metal deposition, Metal coating, Thin film mechanism

1. Introduction

Single-walled carbon nanotubes (SWNTs) [1,2] have attracted much attention as promising materials for next-generation thermal and electrical devices because of their extraordinary thermal and electrical properties[3,4]. While possibilities for single channel devices with an individual SWNT [5] have been extensively explored, bulk SWNT materials in form of mats and films are expected to play an important role in the near future applications due to their handling and cost efficiencies. Among the bulk SWNT materials, vertically aligned SWNT (VA-SWNT) arrays [6-12] have caught great attentions to realize directional bulk transport devices. Particularly, the VA-SWNT grown by alcohol catalytic CVD method [6, 13-15] is known to have high crystallinity. Furthermore, the VA-SWNT films with weak bundles, where a bundle consists of several individual SWNTs with relatively large interbundle-distance, can be synthesized, and thus, the films are expected to sustain properties of individual SWNTs to some extent [16].

Towards device applications of VA-SWNT film as thermal and electrical devices, metal film coating is an important element technology for integration and probing intrinsic properties. Here, studying the metal-SWNT interaction is a primary issue as the contact resistance significantly influences the performance the electrical/thermal conductance in the large mean-free-path systems. Reports on the strong dependence of carbon nanotube transport characteristics on metal type [17,18] have motivated vacuum-evaporation experiments for various metals and deposition conditions [19], which revealed strongly metal-dependent morphologies.

The metal deposition on the individually suspended SWNT was investigated by Zhang et al [19], who coated various metals onto individually suspended SWNTs by electron-beam evaporation and observed the metal morphologies using transmission electron microscopy. It was shown that Ti exhibited better coverage than Au and Al, which was consistent with the interfacial resistances obtained

in the transport measurements [17,18]. The metal dependent nucleation was explained by the surface diffusion rate of adatoms, where the activation energy can be empirically related to the binding energy for the smooth coating surface of an SWNT. From the observed nucleation densities and size of the formed clusters, they have predicted high metal-SWNT binding energies for Ti and Pd, which agrees with a later numerical study. [20].

While the early growth process of the metal layer deposited onto a VA-SWNT film can be understood from the coating of the individual SWNTs, the full coating process is expected to be much more complicated due to the three-dimensional nanostructured surface of the VA-SWNT film and the multistage nature of the metal-layer formation. On depositing metal on top of a VA-SWNT film, each SWNT bundle becomes a nucleation site to form grains along the SWNT. While the coalescence of grains leads to formation of continuous metal layer as in usual metal deposition onto planer substrate [21], the morphology of the VA-SWNT limits inter-bundle metal mass transfer by surface diffusion. This results in two events with significantly different timescales; fast intra-bundle coalescence of clusters by surface diffusion resulting in larger grains, and slow inter-bundle coalescence which requires further growth of the grains and intra-bundle mass transport. This anisotropic and multi-timescale coalescence processes are expected to strongly influence the final smoothness and filling ratio of the metal layer.

In this work, the formation mechanism and resulting structures of four different kinds of VASWNT-metal (Au, Al, Ti and Pd) films were systematically investigated. The smoothness of the VASWNT-metal films depended strongly on the metal species, substrate temperature, deposition rate, and thickness of the deposited layer. This leads us to identify the optimized conditions for obtaining the smooth and uniform metal coating on the VASWNT films.

2. Experiments

2.1. VASWNT synthesis

VASWNTs were synthesized on quartz substrates using the alcohol catalytic chemical vapor deposition (ACCVD) process [6,13-15]. The catalyst was supported on a quartz substrate, which was dip-coated into a Co-Mo acetate solution (metal content 0.01 wt% each, dissolved in ethanol). The catalyst was oxidized by heating the dip-coated substrate in air at 400 °C, and then reduced in a flowing Ar/H_2 mixture (3% H_2, 300 sccm flow rate, 40 kPa) during heating of the growth chamber. When the growth SWNT chamber reached 800 °C, the Ar/H_2 flow was stopped and SWNTs were synthesized by supplying ethanol vapor at 1.3 kPa (10 Torr) until the VASWNT array had reached approximately 5μm in thickness. The average diameter of the VASWNTs was 1.9 nm [6].

2.2. Deposition and characterization of metal films

An evaporative deposition chamber (ULVAC VPC-260F) was used for metal deposition, and characterization was primarily done by SEM observation (JEOL JSM-7000F). Thin films of Au, Al, Ti, and Pd were deposited onto the VASWNT arrays. The deposition rate and thickness of the deposited films were determined using the built-in quartz crystal microbalance, which was calibrated using flat substrates. Since the VASWNT arrays are very porous, it is difficult to define the thickness of the deposited film. Thus we use the 'nominal' film thickness to indicate the thickness of a metal film if it had been deposited onto an atomically flat surface. A resistively-heated target holder allowed the

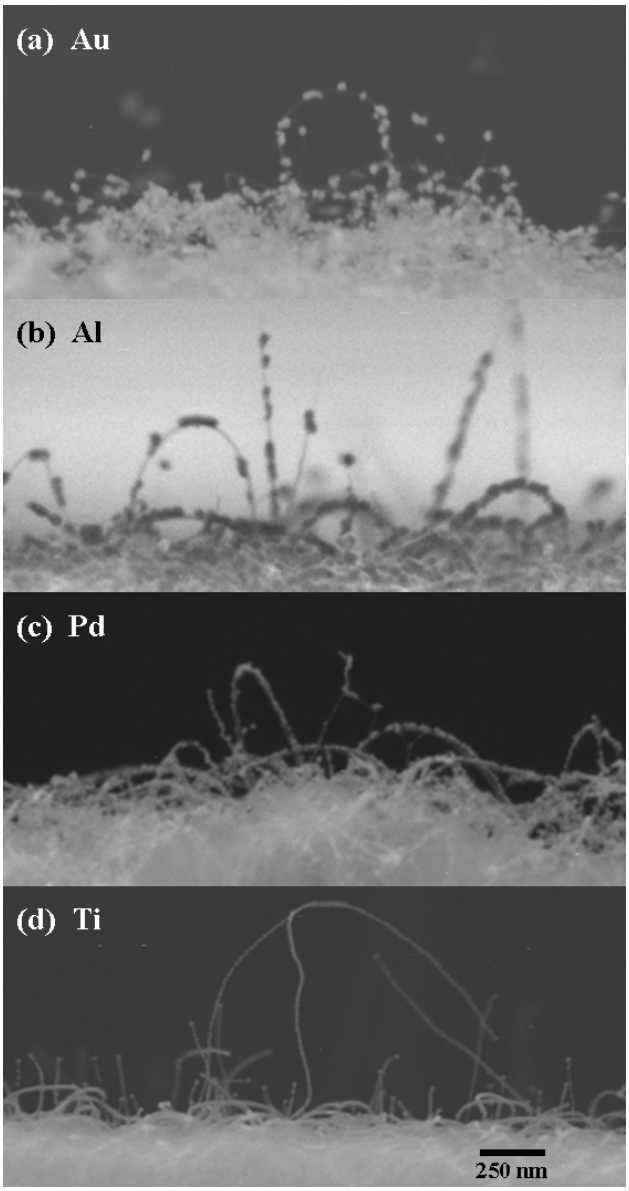

Figure 1. SEM images of VASWNTs coated with a 4 nm layer of: (a) Au, (b) Al, (c) Pd and (d) Ti. Deposition rate was 0.05 nm/s and substrate temperature was 25 °C.

substrate temperature to be controlled between room temperature (approximately 25 °C) and 300 °C. Unless otherwise indicated, the VASWNT target is at room temperature during deposition.

3. Results and Discussion

3.1. Interactions of metals and bundled SWNTs

In order to study the initial stage of the metal deposition and the interactions of the metal adatoms with the SWNTs, 4 nm films of each of the four metal species (Au, Al, Ti, and Pd) were deposited onto the VASWNT arrays with a deposition rate of 0.05 nm/s. The resulting morphologies are shown in the SEM images in Fig. 1. Au and Al (Figs. 1a and 1b) formed discrete clusters on the SWNT bundles, leaving some areas free of metal coating. The observation indicates Au and Al adatoms deposited on the SWNT bundles have diffused along the bundle surface and agglomerated into larger clusters. This suggests small activation energy for surface diffusion of Au and Al adatoms on the SWNT surface, which agrees with the small binding energy of Au- and Al-SWNT [20]. Figure 1d shows the deposition of Ti, which formed a continuous and uniform coating on SWNTs. Deposition of Pd (Fig. 1c) resulted in semi-uniform coverage, with some discontinuous areas. The deposited Ti and Pd appear as small clusters, smoothly connected together along the SWNT bundles. These results are consistent with the work of Zhang *et al.*[19], showing that Ti adatoms exhibit a higher continuity than that of Pd, and much higher than Au and Al, reflecting the order of binding energy to an

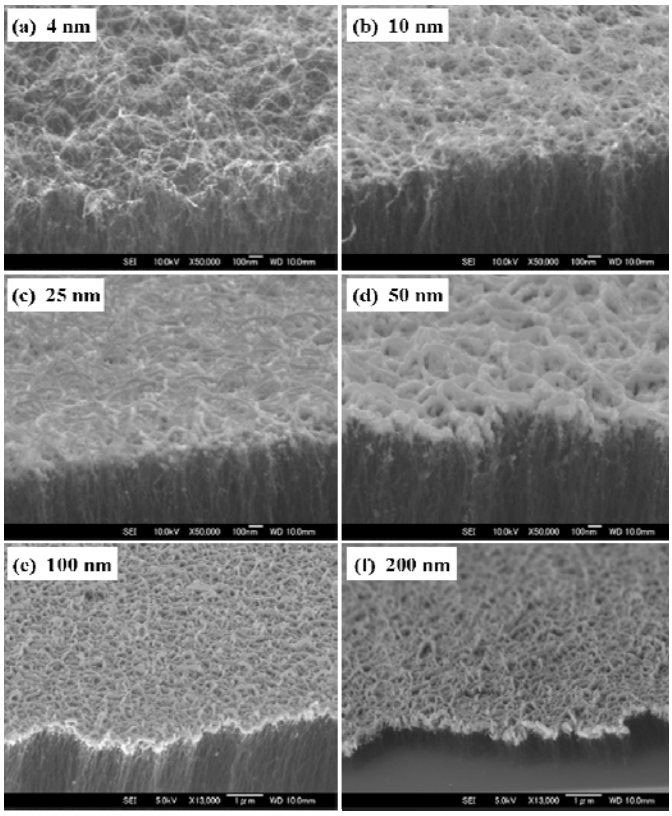

Figure 2. SEM images of VASWNTs coated with Pd films of: (a) 4 nm, (b) 10 nm, (c) 25 nm, (d) 50 nm, (e) 100 nm and (f) 200 nm. Deposition rate was 0.20 nm/s and substrate temperature was 25 °C.

SWNT [20].

3.2. Coating mechanisms of metal film formation on SWNT arrays

To study the coating scenario, Pd films with nominal thicknesses of 4, 10, 25, 50, 100, and 200 nm were deposited onto the VASWNT arrays. The substrate temperature was 25 °C. The deposition rates were 0.05 nm/s for the 4-nm film and 0.20 nm/s for the thicker films. SEM images of the resulting morphologies are shown in Figs. 2a-2f (in order of increasing thickness). As can be seen in Fig. 2a, initially the Pd adatoms form a uniform coating of fine clusters on the SWNT bundles, with some discontinuous regions. Although we can not identify with the current investigation, the nucleation sites are expected to be located at the bundle groves with rich interfacial potential energy. As deposition continues (Figs. 2b-2c), the nucleation sites on the top SWNT layer rapidly approaches a saturation density, and then additional Pd adatoms fill in the gaps between nucleation sites along SWNTs. This results in uniform coating of the SWNTs on the top layer with the coating thickness growing with the amount of deposited metal. Note that at this diffusion controlled stage, the diffusion dominantly takes place along an SWNT bundle since the film morphology limits the inter-bundle mass transport.

The initial growth of clusters along an SWNT bundle leads to formation of larger scale grains by surface diffusion of adatoms and small clusters. As the grain sizes increase with further metal deposition and become larger than the distances between the coated SWNT bundles, the grains begin to coalesce.

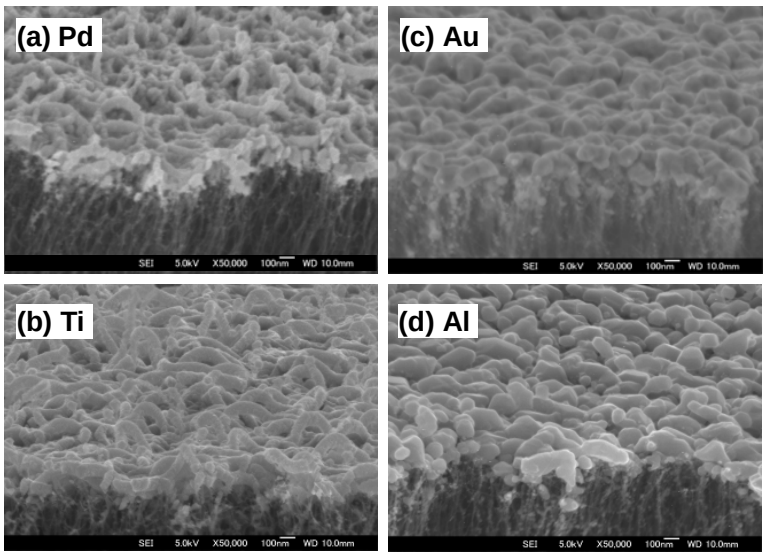

Figure 3. SEM images of different VASWNTs coated with a 100 nm layer of (a) Pd, (b) Ti, (c) Au and (d) Al. Deposition rate was 0.20 nm/s, and substrate temperature was 25 °C.

The rate of increase in the grain size and corresponding decrease in the grain density is influenced by

the deposition condition as discussed later. The coalescence of grains opens mass transport channels among the grains and forms larger network structures of “islands”. Unlike the coalescence of metal islands on planer surface, where a rapid large-scale coalescence of the metal clusters takes place when the island density reached a critical state [21], the coalescence is expected to take place relatively slowly in the current case due to lack of inter-bundle mass transfer. The island coalescence leaves empty channels [21] as shown in Fig. 2d. The channels can be filled with addition of deposition (Fig. 2d-2f), but the process of the adatoms filling-in the empty channels is slow [21] and requires considerable amount of Pd-adatom deposit, particularly for the current “nanopore” system.

The resulting morphology of the metal layer after deposition of 100 nm nominal thickness clearly depends on the metal type as shown in Fig. 3. The deposition rate was 0.20 nm/s for all the cases. The grains of Ti and -Pt films (Figs. 3a and 3b) are elongated along the underlying SWNT bundles, whereas those of the Au and Al films (Figs. 3c and 3d) were largely spheroid clusters, inheriting the characteristics of the initial cluster nucleation (Fig. 1). Although Au and -Al clusters exhibit relatively more frequent inter-bundle bridging with larger grains, they also create more empty channels, which take significantly more amount of deposition to fill and achieve a smooth film. On the other hand, in cases of Ti and Pd, the continuous coverage of individual SWNT-bundle results in more planer film.

3.3. Optimization of the parameters of the coating process of the SWNT-metal films

The smoothness of the SWNT-metal films depended not only on the coated metal types but also on all three experimental parameters: substrate temperature, deposition rate, and metal thickness. In order to find the optimal coating conditions, one of these parameters was changed while two others were kept constant. The effects of the coating parameters on the smoothness of the SWNT-metal films were studied by coating Pd onto SWNT arrays synthesized under the same CVD conditions.

3.4.1 Effect of substrate temperature

The role of substrate temperature was investigated by depositing 100 nm of Au, Al, Ti, and Pd at 25 and 300 °C. The deposition rate was 0.20 nm/s for all the cases (Table 1). Cross-sectional SEM images of the SWNT-Pd, -Ti, -Au and -Al films deposited at room temperature are shown in Figs. 4a-4d, and those deposited at 300 °C in Figs. 5a-5d. At higher substrate temperature, the surface mobility of adatoms increases. While, in the initial "intra-bundle coating" stage, this decreases the nucleation density and increase the cluster size, in the later "inter-bundle coating" stage, it makes the condensation to occur more preferentially at the surface concaves [21]. As a result, the surfaces of the SWNT-metal films are smoother when deposited at 300 °C as seen in Figures 5a-5d. While temperature promotes the film smoothness by enhancing the inter-bundle metal mass transport, excess temperature is expected to decrease the nucleation density and increase the size of clusters at the initial stage, and results in more inter-bundle empty channels. In addition, increasing the temperature allows metal adatoms to penetrate deeper into the SWNT arrays and stick along the SWNT bundles. These suggest that, to efficiently achieve a smooth and uniform metal layer, there exists an optimal window of temperature, which should

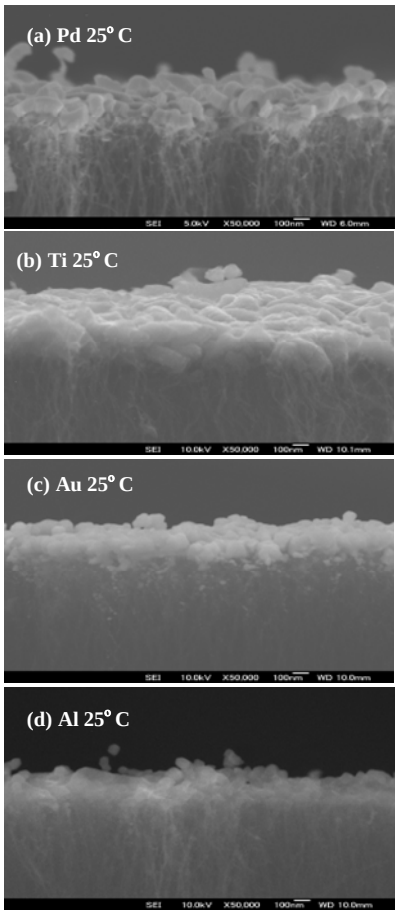

Figure 4. SEM images showing cross sections of VASWNT-metal films from Fig.3 Films are 100nm thick (a) Pd, (b) Ti, (c) Au and (d) Al.

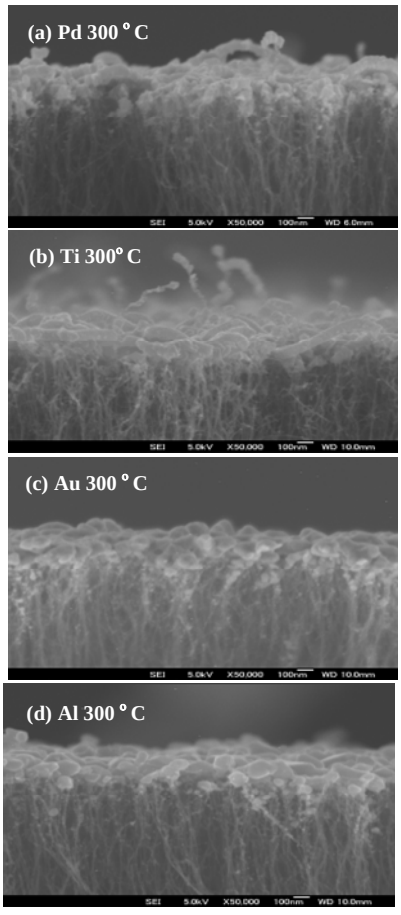

Figure 5. SEM images showing cross sections of VASWNT-metal films deposited with the substrate heated to 300 °C. Film thickness are 100 nm of (a) Pd, (b) Ti, (c) Au and (d) Al, deposited at 0.20 nm/s.

depend on the metal type reflecting the differences in interfacial binding energy and cohesive energy.

3.4.2 *Effect of deposition rate*

To study the effect of the deposition rate on the film smoothness and uniformity, we coated the same amount (100 nm) of Pd onto VASWNT arrays with different coating rates. The resulting films are shown by cross-sectional SEM images in Figs. 6a-6c, where the metal was deposited at room temperature using rates of 0.05, 0.20 and 0.40 nm/s, respectively. The figures show that the grain size is the largest for the 0.20 m/s case and the film is smoothest for the 0.40 m/s case. Note that the visual film thickness is smallest for the highest deposition rate case (0.40 m/s), which suggests the highest filling ratio of the inter-bundle spacing. The results indicate important roles of kinetic energy of the adatoms on the obtained final film morphology. The higher deposition rate gives larger kinetic energy, which firstly enhances the surface mobility, and thus, results in larger cluster in the initial growth along the nanotube-bundle. When the deposition rate is high enough (0.40 m/s), for the given deposition thickness, the kinetic energy enhances the inter-bundle metal mass transfer and therefore the inter-bundle grain coalescence becomes faster resulting in a smoother metal film. In this context, the deposition ratio has similar effect as the previously discussed temperature effect.

Higher deposition rate is also often related to lower diffusion rate due to the stronger binding with the substrate, which would result in more nucleation sites and thus smaller-size clusters. However, the

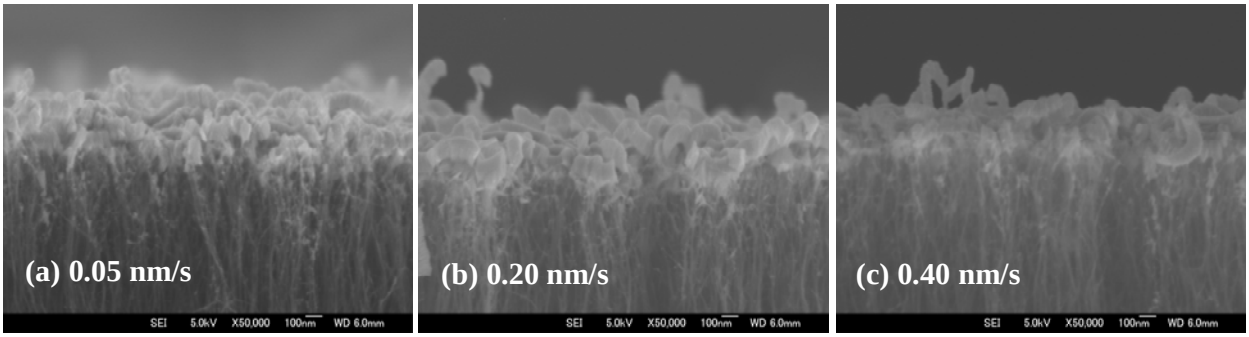

Figure 6. SEM images observed on the side of the SWNT-Pd films with a 100-nm Pd thickness coated under the room temperature at different metal coating rates: (a) 0.05 nm/s, (b) 0.20 nm/s, and (c) 0.40 nm/s.

current result shows the opposite trend, which suggests that the current range of deposition rates are sufficiently smaller than the relaxation rate to thermodynamic equilibrium.

3.4.3 *Effect of the metal thickness on the SWNT-metal films*

The effect of the metal thickness on film smoothness was studied by depositing 50, 100 and 200 nm-thick Pd films on top of VASWNT arrays. The deposition rate was 0.20 nm/s, and the substrate temperature was 25 °C. Top-view and cross-sectional SEM images of SWNT-Pd films with thicknesses of 50, 100, and 200 nm are shown in Figs. 7a-7c (top) and 7d-7f (side), respectively. In Figs. 7a/7d, coating thickness of 50 nm of Pd is not sufficient to fill-in the empty spaces in the SWNT-Pd films. When more Pd is deposited, the empty channels are mostly filled (Fig. 7b), and larger Pd islands are formed on the top of the array (Fig. 7e). Figure 6f shows that with a thicker Pd layer, cubic Pd particles are formed, resulting in a smooth surface of 200 nm SWNT-Pd film. For low resistance contact, it is important that the internal empty channels are filled. The result shows, for Pd deposition at room temperature and realistic range of deposition rate, unusually thick deposition thickness of about 200 nm

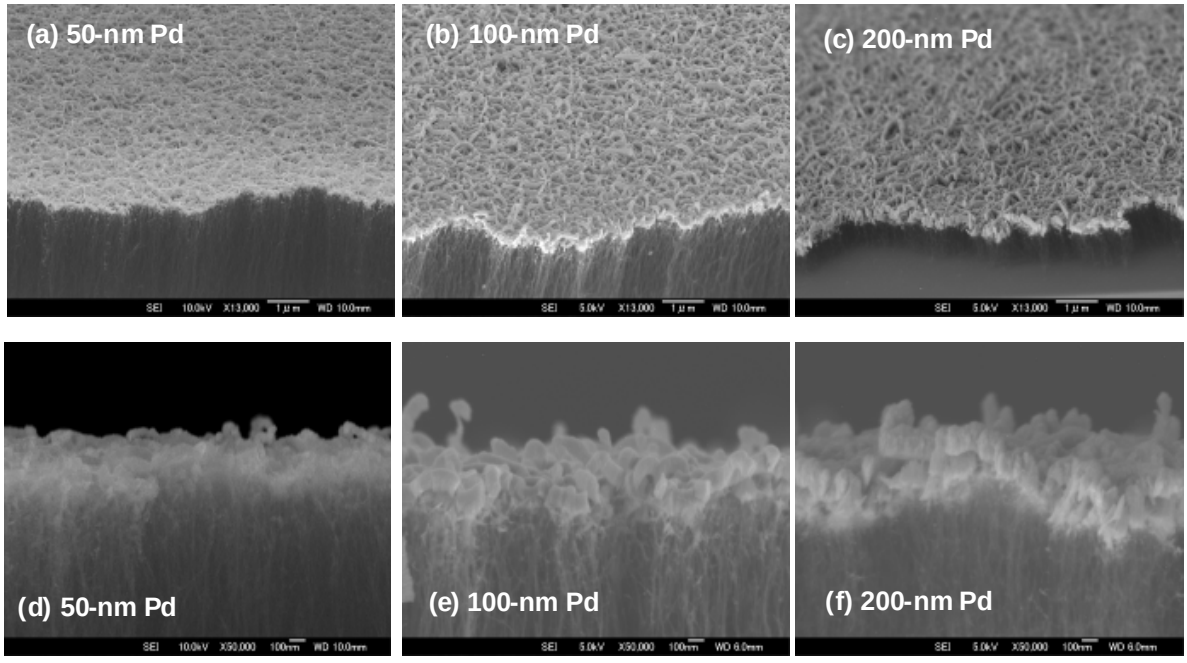

Figure 7. SEM images of the top and side of VASWNT-Pd films. Pd thickness are (a) and (d) 50 nm; (b) and (e) 100nm, and (c) and (f) 200 nm. Deposition rate was 0.20 nm/s and the substrate temperature was 25 °C.

is required to achieve a smooth surface. While this is usually a very slow process involving internal mass diffusion than the fast surface diffusion, the current nanopore system with limited inter-bundle mass transport is expected to require even more time and deposition for the internal film structure to saturate.

4. Conclusions

Thin films of four different metals (Au, Al, Ti, and Pd) were deposited onto the VASWNT arrays by an evaporative deposition method. By systematically adjusting various parameters, the growth process and morphologies of the thin metal films were investigated. Depending on the metal species, continuous films (for Ti and Pd) or discrete clusters (for Au and Al) formed on the SWNT bundles during the early stage of the coating process reflecting the differences in the binding energy. In the later stage of the coating process, although Au and -Al clusters exhibit faster inter-bundle bridging due to the growth of large grains, they also create more empty channels, which take significantly more amount of metal deposition to fill and achieve a uniform film. On the other hand, Ti and Pd with stronger binding energy show better coverage of an individual SWNT-bundle but the inter-bundle bridging takes place relatively slowly. Therefore, the deposition efficiency for smooth coating layer is determined by the balance of the intra-bundle and inter-bundle coating. We have indentified the deposition parameter window, within a typical range in vacuum metal deposition, for Pd that efficiently realizes a smooth metal layer. The current results also provide guidelines to optimize the coating efficiency for other metal types.

REFERENCES

(1) Iijima, S. *Nature* **1991**, 354, 56.

(2) Iijima, S.; Ichihashi, T. *Nature* **1993**, 363, 603.

(3) Dresselhaus, M.S.; Dresselhaus, G.; Eklund, P.C. *Sci. Full. Carbon Nanotube*, Academic Press, San Diego, **1996**.

(4) Jorio, A.; Dresselhaus, G.; Dresselhaus, M. S.; Topics in applied physics: carbon nanotubes, advanced topics in the synthesis, structure, properties and applications, Springer-Verlag **2008**.

(5) Tans, S.J.; Verschueren, A.R.M.; Dekker, C. *Nature* **1998**, 393, 49.

(6) Murakami,Y.; Chiashi, S.; Miyauchi, Y.; Hu, M.; Ogura, M.; Okubo, T.; Maruyama, S. *Chem. Phys. Lett.* **2004**, 385, 298.

(7) Hata, K.; Futaba, D. N.; Mizuno, K.; Namai, T.; Yumura, M.; Iijima, S. Science **2004**, 306, 1362.

(8) Zhang, G.; Mann, D.; Zhang, L.; Javey, A.; Li, Y.; Yenilmez, E.; Wang, Q.; McVittie, J. P.; Nishi, Y.; Gibbons, J.; Dai, H. Proc. Natl. Acad. Sci. **2005**, 102, 16141.

(9) Zhong, G.; Iwasaki, T.; Honda, K.; Furukawa, Y.; Ohdomari, I.; Kawarada, H. Jpn. J. Appl. Phys. **2005**, 44, 1558.

(10) Eres, G.; Kinkhabwala, A. A.; Cui, H.; Geohegan, D. B.; Puretzky, A. A.; Lowndes, D. H. J. Phys. Chem. B **2005**, 109, 16684.

(11) Xu, Y.-Q.; Flor, E.; Kim, M. J.; Hamadani, B.; Schmidt, H.; Smalley, R. E.; Hauge, R. H. J. Am. Chem. Soc., **2006**, 128, 6560.

(12) Noda, S.; Hasegawa, K.; Sugime, H.; Kakehi, K.; Zhang, Z.; Maruyama, S.; Yamaguchi, Y. Jpn. J. Appl. Phys. **2007**, 46, L399.

(13) Maruyama, S.; Kojima, R.; Miyauchi, Y.; Chiashi, S.; Kohno, M. *Chem. Phys. Lett.* **2002**, 360, 229.

(14) Maruyama, S.; Einarsson, E.; Murakami, Y.; Edamura, T. *Chem. Phys. Lett.* **2005**, 403, 320.

(15) Hu, M.; Murakami, Y.; Ogura, M.; Maruyama, S.; Okubo, T. *J. Catal.* **2004**, 225, 230.

(16) Einarsson, E.; Shiozawa, H.; Kramberger, C.; Ru1mmeli, M. H.; Gru1neis, A.; Pichler, T.; Maruyama S. J. Phys. Chem. C **2007**, 111, 17861.

(17) Dai, H.; Kong, J.; Zhou, C.; Franklin, N.; Tombler, T.; Cassell, A.; Fan, S.; Chapline, M. *J. Phys. Chem.* **1999**, 103, 11246.

(18) Zhou, C.; Kong, J.; Dai, H. *Phys. Rev. Lett.* **2000**, 84, 5604.

(19) Zhang, Y.; Franklin, N.W.; Chen, R.J.; Dai, H. *Chem. Phys. Lett.* **2000**, 331, 35.

(20) Durgun, E.; Dag, S.; Bagci, V. M.; Gulseren, O.; Yildirim, T.; Ciraci, S. Phys. Rev. B **2003**, 67, 201401.

(21) Chopra, K.L. *Thin Film Phenomena* **1979**, Krieger, 137.

FIGURE CAPTIONS

Figure 1. SEM images of VASWNTs coated with a 4 nm layer of: (a) Au, (b) Al, (c) Pd and (d) Ti. Deposition rate was 0.05 nm/s and substrate temperature was 25 °C.

Figure 2. SEM images of VASWNTs coated with Pd films of: (a) 4 nm, (b) 10 nm, (c) 25 nm, (d) 50 nm, (e) 100 nm and (f) 200 nm. Deposition rate was 0.20 nm/s and substrate temperature was 25 °C.

Figure 3. SEM images of different VASWNTs coated with a 100 nm layer of (a) Pd, (b) Ti, (c) Au and (d) Al. Deposition rate was 0.20nm/s, and substrate temperature was 25 °C.

Figure 4. SEM images showing cross-sections of VASWNT-metal films from Fig. 3. Films are 100 nm thick (a) Pd, (b) Ti, (c) Au and (d) Al.

Figure 5. SEM images showing cross-sections of VASWNT-metal films deposited with the substrate heated to 300 °C. Film thicknesses are 100 nm of (a) Pd, (b) Ti, (c) Au and (d) Al, deposited at 0.20nm/s.

Figure 6. SEM images observed on the side of the SWNT-Pd films with a 100-nm Pd thickness coated under the room temperature at different metal coating rates: (a) 0.05nm/s, (b) 0.20nm/s, and (c) 0.40nm/s.

Figure 7. SEM images of the top and side of VASWNT-Pd films. Pd thicknesses are (a) and (d) 50 nm, (b) and (e) 100nm, and (c) and (f) 200 nm. Deposition rate was 0.20nm/s, and substrate temperature was 25 °C.

TABLES

Table 1. Summary of deposition conditions

Metals	Nominal thickness (nm)	Coating rate (nm/s)	Substrate temperature (°C)
	Section 3.1		
Au	4.0	0.05	25
Al	4.0	0.05	25
Ti	4.0	0.05	25
Pd	4.0	0.05	25
	Section 3.2		
Pd	**4**	0.05	25
Pd	**10**	0.20	25
Pd	**25**	0.20	25
Pd	**50**	0.20	25
Pd	**100**	0.20	25
Pd	**200**	0.20	25
	Section 3.3		
Au	100	0.20	**25**
Au	100	0.20	**300**
Al	100	0.20	**25**
Al	100	0.20	**300**
Ti	100	0.20	**25**
Ti	100	0.20	**300**
Pd	100	0.20	**25**
Pd	100	0.20	**300**
Pd	100	**0.05**	25
	100	**0.20**	25
	100	**0.40**	25
Pd	**50**	0.20	25
	100	0.20	25
	200	0.20	25